Observations of Naturally Occurring Lightning with Event-Based Vision Sensors

Imogen Jones[1], Julia Zoe Hallgren[2], Nicholas Owen Ralph[2], Alexandre Marcireau[2], and Gregory Cohen[2]

[1]Affiliation not available
[2]International Centre for Neuromorphic Systems (ICNS), Western Sydney University

February 23, 2024

Abstract

Lightning is an impressive, widespread natural phenomenon, yet many questions about its physics remain unanswered due to its extreme speed, transience, and high energy. These intrinsic characteristics make optical observations capturing its formation, propagation, and discharge challenging with conventional optical cameras. Furthermore, optical sensors with extremely high-speed frame rates and high dynamic ranges are needed. While high speed cameras have been used to capture lightning, their lack of portability, high cost and high data storage requirements can limit lightning research. To address these challenges, the use of neuromorphic technologies, inspired by the sensing and data processing mechanisms of biological photoreceptors, offers a unique approach. Event-based vision sensors offer low latency, less power than a conventional camera, and have sensing capabilities that operate across a dynamic range of over 120dB. This paper demonstrates the effectiveness of Event-Based Vision Sensor in lightning research by presenting data collected during a full lightning storm and provides examples of how event-based data can be used to interpret various lightning features. We used a Prophesee Gen4 Event-Based Vision Sensor to record a thunderstorm over a fifty-minute span on 24 January 2023, from Western Sydney, New South Wales, Australia. During this observation, we recorded numerous Cloud-to-Ground and Cloud-to-Cloud lightning strikes. To assess the Event-Based Vision Sensor's effectiveness in capturing commonly observed lightning features, we used custom algorithms and in-house post-processing software was used to analyze and interpret the data. We conclude that the Event-Based Vision Sensor has the potential to improve high-speed imagery due to its lower cost, data output, and ease of deployment, ultimately establishing it as an excellent complementary tool for lightning observation.

Observations of Naturally Occurring Lightning with Event-Based Vision Sensors

Imogen Rae Jones, Julia Zoe Hallgren, Nicholas Owen Ralph, Alexandre Marcireau, Gregory Cohen

[1]International Centre for Neuromorphic Systems (ICNS), Western Sydney University, Werrington, New South Wales, Australia

Key Points:

- Event-based vision sensors record changes in contrast in a scene at high speed and low data rate, making them ideal for recording lightning
- Presented here are observations of lightning with event-based vision sensors, plus data analysis techniques
- Several known features of lightning were clearly observed in the data presented here

Corresponding author: Imogen Jones, `I.Jones2@westernsydney.edu.au`

Abstract

Lightning is an impressive, widespread natural phenomenon, yet many questions about its physics remain unanswered due to its extreme speed, transience, and high energy. These intrinsic characteristics make optical observations capturing its formation, propagation, and discharge challenging with conventional optical cameras. Furthermore, optical sensors with extremely high-speed frame rates and high dynamic ranges are needed. While high speed cameras have been used to capture lightning, their lack of portability, high cost and high data storage requirements can limit lightning research. To address these challenges, the use of neuromorphic technologies, inspired by the sensing and data processing mechanisms of biological photoreceptors, offers a unique approach. Event-based vision sensors offer low latency, less power than a conventional camera, and have sensing capabilities that operate across a dynamic range of over 120dB. This paper demonstrates the effectiveness of Event-Based Vision Sensor in lightning research by presenting data collected during a full lightning storm and provides examples of how event-based data can be used to interpret various lightning features. We used a Prophesee Gen4 Event-Based Vision Sensor to record a thunderstorm over a fifty-minute span on 24 January 2023, from Western Sydney, New South Wales, Australia. During this observation, we recorded numerous Cloud-to-Ground and Cloud-to-Cloud lightning strikes. To assess the Event-Based Vision Sensor's effectiveness in capturing commonly observed lightning features, we used custom algorithms and in-house post-processing software was used to analyze and interpret the data. We conclude that the Event-Based Vision Sensor has the potential to improve high-speed imagery due to its lower cost, data output, and ease of deployment, ultimately establishing it as an excellent complementary tool for lightning observation.

Plain Language Summary

Event-based vision sensors (EBVS) are a unique type of optical sensor that complements conventional cameras to observe the features of lightning. Instead of capturing an image of lightning frame by frame, the EBVS detects changes in contrast within a scene. They offer high-speed observations but with improved contrast, which is especially useful for bright phenomena like lightning. The EBVS's ability to only record changes in brightness significantly reduces the amount of data generated compared to typical high-speed cameras. As a result, they can capture an entire storm event. Here we show that EBVS has the potential to capture lightning images with features that were previously difficult to capture using regular high-speed cameras.

1 Introduction

There are many unanswered questions regarding the physics of lightning, such as how lightning is initiated within thunderclouds, the physical mechanisms governing the propagation of diverse types of lightning leaders, and what determines the direction in which a lightning leader travels (Dwyer & Uman, 2014). To extend our understanding of the physical processes of lightning, novel approaches to uncovering previously unresolved lightning features are required to address these outstanding questions. Existing observations use a variety of methods across different spectral ranges, including radio, visual, and x-ray spectral ranges (Biagi et al., 2010; Jiang et al., 2021; Wang et al., 2022; Rakov et al., 2022; Zeng et al., 2016; Walker & Christian, 2017, 2019; B. M. Hare et al., 2020). High-speed cameras are often used to capture features of lightning due to their rapid frame rate (Biagi et al., 2009, 2010; Saba et al., 2006; Hill et al., 2011; Campos et al., 2014; Qi et al., 2019; Wu et al., 2022; Petersen & Beasley, 2013; Qi et al., 2016). However, they have some drawbacks, including the high cost of the cameras themselves and the generation of large data outputs which make continuous recording over prolonged periods difficult (Campos et al., 2014; Saraiva et al., 2014; Qi et al., 2019). We demonstrate the use of an alternative sensor with high temporal resolution and wide dynamic range to observe lightning, and its effectiveness in capturing features of lightning.

Event-based vision sensors (EBVS) are CMOS silicon-based imaging sensors, whose pixels contain special analog circuitry that allows them to operate asynchronously and independently from one another. Each pixel operates as a temporal contrast sensor, emitting data only in responses to changes in contrast, which usually results from changes in brightness in a scene (Gallego et al., 2020). Unlike conventional cameras, these sensors do not emit frames, nor do they make use of a constant sampling rate. As a result, these sensors have no exposure times or frame rates, instead each pixel outputs an "event" whenever the log intensity of the brightness change at the pixel exceeds certain thresholds (Gallego et al., 2020). These thresholds, or bias settings, are user-configurable chip-wide parameters that control the sensitivity of the sensor to both positive and negative changes in contrast. These values can be asymmetrical, allowing for greater sensitivity for contrast changes in one direction over the other.

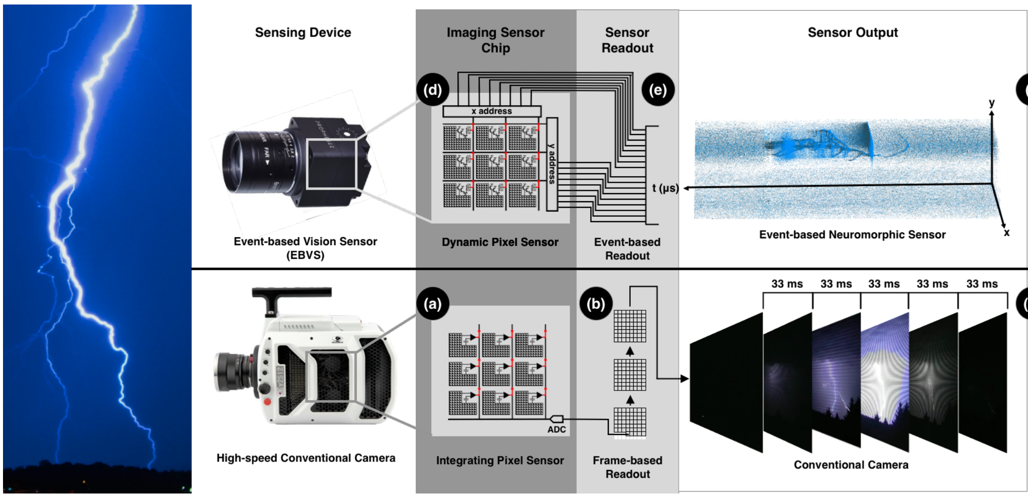

Figure 1: Diagram illustrating the differences between a conventional imaging sensor and an event-based vision sensor. The above figure shows the information flow through a representation of a conventional cameras (bottom row) and an neuromorphic event-based camera (top row). In a conventional camera, such as the high-speed camera, a large-format CMOS or CCD sensor is used to synchronously capture a visual representation of the scene. The pixels inside these cameras integrate the photocurrent and allow it to read out sequentially, as shown in (a). The output of these cameras is digitized using an ADC and assembled into conventional image frames, as shown in (b). These frame are generated at the frame rate at which the camera is sampled, resulting in discrete visual representations of the scene separated uniformly in time, as shown in (c). By contrast, the EBVS contains a sensor with specialized analog pixels that implement a temporal contrast detector, as shown in (d). These pixels do not output frames, but rather emit a stream of contrast change events only when they occur, each with microsecond timing. This is illustrated in (e), showing the continuous output of the sensor, rather than the assembly of discrete frames. The output of the EBVS, shown in (f) is fundamentally different from the frames generated by conventional camera. The output is a sparse spatiotemporal signal, providing many of the benefits of the high-speed camera by breaking the relationship between frame rate and the volume of data produced.

The pixels in an EBVS are fabricated using conventional silicon technologies, making their spectral response similar to conventional CMOS and CCD cameras. Unlike conventional sensors, the photocurrent from the photoreceptor is not integrated but rather clamped using a set of transistors to produce a signal proportional to the log of the photocurrent. This signal is then passed through an temporal differencing detector which compares it to the signal last used to generate an event. This difference is finally compared, via two comparators, to the positive and negative threshold biases, which will signal that an change event has occurred.

Instead of a conventional frame readout, the EBVS has an arbiter that is responsible for checking and retrieving events generated by each pixel. Once an event is detected at a pixel, the pixel itself is reset (causing the temporal differencing detector to change the stored threshold). The location and polarity of the change is then combined with an absolute timestamp to indicate the moment at which the event occurred. These four values $[x, y, t, p]$ comprise an event from the sensor, in which x and y represent the spatial location of the pixel within the sensor array, p is a binary value indicating whether the event was a positive change in contrast (ON event) or a negative change in contrast (OFF event), and t is the timestamp at which the event occurred (usually provided in μ). This operation is described in detail in (Gallego et al., 2020).

In addition to the bias settings that control the sensitivity to contrast changes, the sensor also provides other bias settings that control the responsiveness, speed, bandwidth, and gain of the analog circuit within each pixel, allowing for the sensor to be tuned for specific tasks.

EVBS sensors produce data only in response to changes, necessitating the need for data-driven systems. In place of a constant frame rate, the pixels only produce data in response to changes. Therefore, it is possible to achieve the equivalent of a high-speed camera performance without the need to sample each pixel at extremely high speeds. Therefore, if an EBVS is stationary, it ideally produces no data output where there are no detectable changes in brightness in a scene, suppressing redundant information such as static and unchanging background features. As a result, the data rate becomes activity-driven and can capture high-speed phenomena with high temporal resolution without the need for external triggering.

The EBVS offers several advantages over conventional sensors. Data rate and downstream computational load can be significantly reduced with the EBVS's highly efficient frame-free operation. Processing of event data is different to frame-based image processing as there are no regular sampling intervals, color channels, or light intensity information. Therefore, event data also requires specialized software to visualize the data for interpretation.

These features make the EBVS an excellent candidate for use in the study of lightning. The purpose of this paper therefore, is:

1. to demonstrate the capabilities of EBVSs in capturing the features of lightning, and
2. to demonstrate methods of visualizing event data that may be useful in interpreting features of lightning.

We demonstrate the visualization of event data through event-rate plots, static plots with just 'on' and 'off' events, and plots with temporally colour coded information. Further, to show what can be achieved through analysis of event-based data for lightning, we use a published, event-based tracking algorithm to perform analysis on the data and to extract and model the relative speeds of lightning leaders. We also provide an overview of improvements to an EBVS observing system that may enhance future observations and results.

1.1 Features of Lightning and Nomenclature

The nomenclature of lightning features varies across the literature. Accordingly, in this paper, we will focus primarily on the most common and recent definitions previously established to describe the features we demonstrate.

In this paper, lightning will be categorized as either cloud-to-ground (CG) or cloud-to-cloud (CC) strikes (Dwyer & Uman, 2014). During CG strikes, a downward lightning leader propagates from the cloud to the ground (Dwyer & Uman, 2014), following the electric field gradient through the conductive air (Dwyer & Uman, 2014; Ding & Rakov, 2022; Jiang et al., 2015). As the leader approaches the ground or nearby objects, it induces an upward streamer or leader of opposite polarity (Dwyer & Uman, 2014). While our focus is not on these upward streamers or leaders, it is speculated that the characteristics of the downward leader's propagation significantly influence upward leaders, and in turn, the attachment processes involved (Jiang et al., 2015). This necessitates further investigation of leader propagation.

Negative downward leaders usually have a distinctive stepped pattern, leading to their classification as 'negative stepped leaders', which has been observed in both natural and triggered lightning strikes (B. M. Hare et al., 2020; Biagi et al., 2014; Wang et al., 2019). Many studies rely on triggered lightning techniques to understand the behavior of natural lightning as in these cases the location and time of the lightning leaders can be easily determined (Cai et al., 2022; Wang et al., 2022, 2019; Biagi et al., 2014; Zhang et al., 2014; Gamerota et al., 2014). As the downward negative stepped leaders propagate, they typically branch out across the sky. CC lightning, whilst not as well-documented, is also seen to have negative stepped leaders that follow the same behaviors. As the negative leader branches extend in a step-like manner, each step generates a travelling wave of moving positive charge from the branch tip along the channel (Ding & Rakov, 2022). While negative stepped leaders are extensively documented, the exact nature and mechanism of the phenomenon have yet to be fully understood (Lowke & Szili, 2022; Wang et al., 2022; Ding & Rakov, 2022). Moreover, a negative stepped leader with pronounced branching creates a complex and continuously changing electric field pattern, leading to the formation of complex branching structures (Ding & Rakov, 2022). Branches at higher altitudes may decay faster than those formed later, as they may lose connection with the main channel (Ding & Rakov, 2022).

After the attachment process, the lightning leader forms a highly conductive hot plasma channel through which the return stroke traces (Liang et al., 2014). In CG lightning, the return stroke is an extremely rapid and bright current wave typically described as travelling up the main plasma channel, without branching as it propagates, even if the downward leader had extensive branching (Liang et al., 2014). The speed of the return stroke cannot be directly measured, although its current wave has been estimated to be between 1/3 and 2/3 of the speed of light (Liang et al., 2014; Zhou et al., 2019). Additionally, the optical wave has been found to exhibit varying speeds throughout its propagation, making capturing the return stroke challenging (Liang et al., 2014; Zhou et al., 2019).

Following the initial return stroke that neutralizes charges within the channel, secondary leaders known as 'dart leaders' have been observed travelling through the dormant remnant path, initiating a secondary return stroke (Thiemann & Gasiewski, 2014; Gamerota et al., 2014; Cai et al., 2022; Wang et al., 2022). Despite extensive research, the mechanisms by which the dormant plasma channel induces secondary leaders remain a mystery (B. M. Hare et al., 2023). Nevertheless, it is generally accepted that remnants of the hot plasma channel provide a conductive path for the dart leader to follow (Thiemann & Gasiewski, 2014; Gamerota et al., 2014; Cai et al., 2022). A successful dart leader may then induce a secondary return stroke, leading to the occurrence of multiple return strokes

(Gamerota et al., 2014), a process which may continue until no new dart leader is initiated (Dwyer & Uman, 2014; Yuan et al., 2020; Shi et al., 2019; Filik et al., 2021).

Multiple return strokes have been observed in both positive and negative lightning discharges, occurring in both natural and triggered lightning events (Yuan et al., 2020; Shi et al., 2019; Filik et al., 2021). We will refer to an unsuccessful lightning strike as a leader that does not result in a return stroke. If the dart leader remains in the cloud and is unsuccessful in initiating a return stroke, a different terminology is typically applied (Jensen et al., 2020). There is variation in terminology surrounding dart leaders that fail to reach the ground; some papers refer to them as 'K leaders', while more recent publications use the term 'recoil leaders' (Jensen et al., 2020; Jiang et al., 2021; Huang et al., 2021; Cruz et al., 2022; Liu et al., 2021; B. M. Hare et al., 2023). Therefore, in this context, we will use the term 'recoil leaders' to encompass dart leaders that are unsuccessful, while acknowledging that their phenomenon has been observed to align with dart leaders (Jensen et al., 2020).

2 Materials and Methods

2.1 Equipment and Data Collection

On 24th of January 2023 at 19:27 AEST (08:27 UTC), a thunderstorm was observed from a Western Sydney University campus in Werrington, New South Wales, Australia. A Prophesee GEN4 EBVS was used, which has 1280 x 720 pixels, with a pixel pitch of 5 microns. Further information on the specifications of this camera can be obtained from Prophesee on request at their discretion. A commercial off-the-shelf Fuji 12mm telephoto lens was used for data collection. The EBVS was controlled with a laptop via USB and software developed by ICNS. The EBVS was placed next to a window pointed westerly towards the incoming storm and left to record until it passed over the top of the building, approximately 50 minutes later. A total of 22.95GB of data was collected.

2.2 Data Analysis

2.2.1 Event-Rate Plots and Rainbow Plots

Various software was written in the programming language Python3 to assist in the visualization of the lightning captured in our observations. The software takes the output of the EBVS and plots it on an x,y plane over time. Typically, there is one color for "on" events and one color for "off" events, which in this paper are yellow and blue, respectively.

Presented in this work are 'event-rate plots', which show the number of events per second over time. While searching through data for lightning, one can easily detect a significant increase in events per second, which, in this case, is an indication that lightning occurred. Further, one may ascertain some arbitrary or relative measure of intensity of features such as return strokes.

It is possible to visualize event data in a manner similar to a conventional image frame by binning all events that occur over a fixed time interval and accumulating them from each pixel. This forms a 2D histogram that counts the number of events per pixel and produces an output that resembles a conventional 2D image frame. Colored plots were produced, which visualize the strike as it would appear in a stack of frame-based images, but show events as colors. The program uses color gradients to discern between the first and last events that appear in the scene. The in-house software developed to create figures of lighting uses both on and off events to produce these colored images, which we will henceforth refer to as "rainbow plots". We present event-rate plots and rainbow plots.

2.2.2 Tracking Lightning Leaders

Given the data presented in this paper was only captured with a single EBVS, absolute speeds of leaders cannot be determined by tracking. However, we can measure the 2D projected speed on the image plane in pixels per unit time and infer relative speeds of leaders in relation to each other. Here we demonstrate a simple tracking algorithm that automatically analyses the motion of lightning phenomena to estimate their relative speeds and the motion of surrounding phenomena. The spatio-temporal nature of event-based data is very well suited to performing high-speed tracking. Specifically, the high temporal resolution of events results in highly frequent position updates for trackable targets. For he purposes of this paper, we define tracking as the challenging process of estimating the state of an unknown and time varying number of targets among noise and clutter based on measurements from a sensing system.

In this paper, we approached the problem of tracking lightning leaders using the first-principles Global Nearest Neighbour (GNN) tracker (Blackman & Popoli, 1999) as a simple and well-established tracking algorithm. We also use a 'tracking-by-detection' framework to sequentially detect then track lightning leaders to estimate their motion. Detection is performed using DBSCAN clustering (Ester et al., 1996), where track-able lightning leaders are assumed to be correlated with spatio-temporal consistent and coherent features in the event-stream. This detection via clustering is performed synchronously on a 'center-surround spiking filtered' window of events in 50 μs intervals. Figure 2 provides an overview of the processing pipeline of the tracker. A detailed description of how the tracking system works is given in the Supporting Information.

A track measurement is any observational information of a target, which can range from raw sensor outputs of a given target characteristic such as position. In tracking-by-detection, the output of a detector such as a clustering or filtering algorithm is also considered a track measurement. To estimate the state of a target, track measurements are associated to known or potential targets, which are used to infer desired target state qualities including position, speed and acceleration using Bayesian techniques such as Kalman Filtering (Kalman, 1960), Particle Filtering (Del Moral, 1997) or a general Markov-Bayes recursion (Ralph et al., 2022). Tracking algorithms generally use a track manager to maintain unique track identifiers and the life cycle of tracks. The track life cycle begins when a new measurement is received and an unconfirmed track is initialized, progressing to track confirmation when the track has high confidence (i.e. it has produced many position measurements) and track pruning when the target has disappeared or left the field of interest. The core distinguishing factor of most tracking algorithms is their approach to the data association, where measurements are assigned to the tracks which they most likely represent.

3 Results

The EBVS recorded a lightning storm continuously for approximately 50 minutes, resulting in 12.3GB of uncompressed data being recorded. 33 CG and 16 CC strikes were clearly visible in the data. Other "flashes" were observed, but any structure within those flashes was obscured by cloud, or the strike occurred out of frame. Leader propagation was shown in all observations of CG and CC strikes captured throughout the observing campaign. Distinct leader propagation and return stroke initiation was present in several strikes. Dart leaders were also observed, some of which initiated multiple return strokes within a lightning flash. Given the number of strikes captured, we have chosen some outstanding examples of both CG and CC strikes with distinctive features to present here, including an example of a negative stepped branched leader with a single return stroke, multiple return stroke and no return stroke. Event-rate plots and rainbow plots were produced for these examples, followed by a demonstration of the use of the tracking algorithm for one strike.

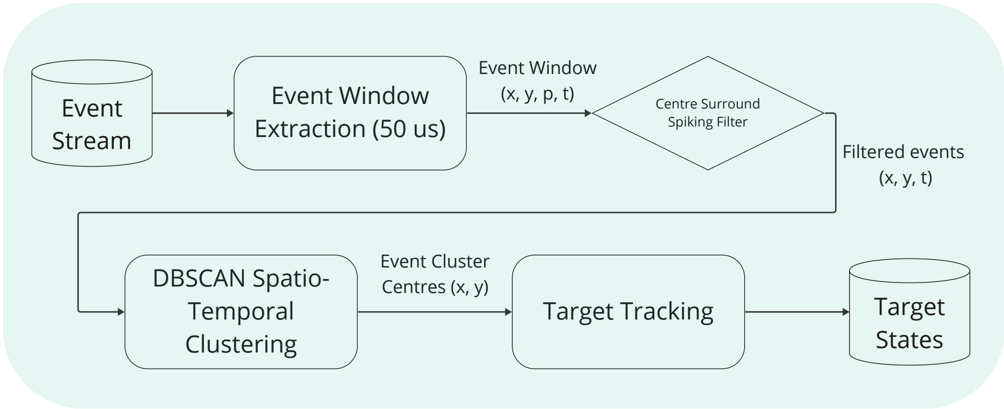

Figure 2: Abstracted overview of the proposed lightning feature tracking algorithm pipeline from raw event-stream data to estimated target position and velocity states.

3.1 Event-Rate Plots

To demonstrate event-rate plots, 3 different sequences of lightning flashes captured by the EBVS are provided. During the thunderstorm, at 19:46:31, the EBVS recorded a negative stepped leader propagating and branching across the sky in a CG flash (Figure 3). Later, at 19:49:47, a CG lightning flash, that was initiated by a negative stepped leader and had multiple return strokes, was recorded (Figure 4). The EBVS then captured, at 19:51:59, a small sequence of discharge events that reionize channels from an unsuccessful branched negative stepped leader (Figure 5). Rainbow plots are provided for two of the flashes as visual aids to complement the event-rate plots.

At around 19:46:31, a CG negative branched stepped leader was captured, figure 3. This leader initiated a single return stroke with no apparent reionization of the plasma channel. Corresponding to the single return stroke, the event-rate plot of this flash, figure 3a, has one peak. This peak has a magnitude of around 10^9 events, where the initial background noise of the camera averages at 10^6 events. Figure 3a shows a gradual increase in events corresponding to leader branching, followed by a rapid spike during the return stroke, and finally, a gradual decrease. The propagation of the leader and its branches before the return stroke is visually represented with a rainbow plot in Figure 3b. Although event rates do increase with leader propagation and branching, there remains a clear distinction between the leader and its branches, and the return stroke, as evidenced by the magnitude change in event rates.

A CG negative stepped lightning leader with multiple subsequent return strokes was captured at 19:49:47. The corresponding video of the lightning flash sequence, whilst not shown here, depicted several return strokes and dart leader through the same channel over 0.357 seconds. While it is difficult to visualize this without the video, it can be shown in the event-rate plot, 4. The main channel is momentarily dormant after the initial return stroke but becomes luminous again multiple times with varying event magnitude. This lightning flash closely reaches its peak magnitude of 10^9 events 3 times. Remaining peaks have magnitudes between 10^8 and 10^9 events per second. The series of return stokes of flash in figure 4 is temporally separated by two main sequences. The first sequence, following the initial negative stepped leader, has clear peaks that can be correlated to return strokes. A second sequence of peaks occurs after 0.285600 seconds when charge re-enters the main channel as an additional lightning flash is initiated outside the EBVS's frame. Furthermore, the less distinct peaks of the second sequence are attributed to an increase of noise from the secondary strike outside the camera's frame. Between

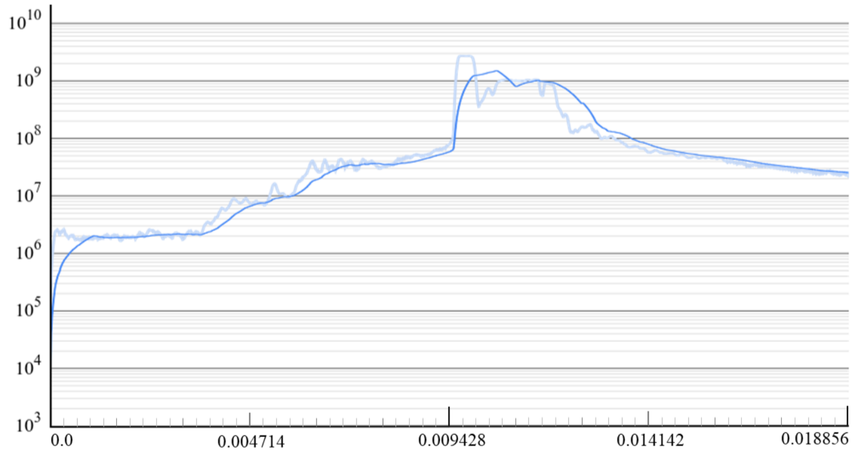

(a) Event over time (seconds)

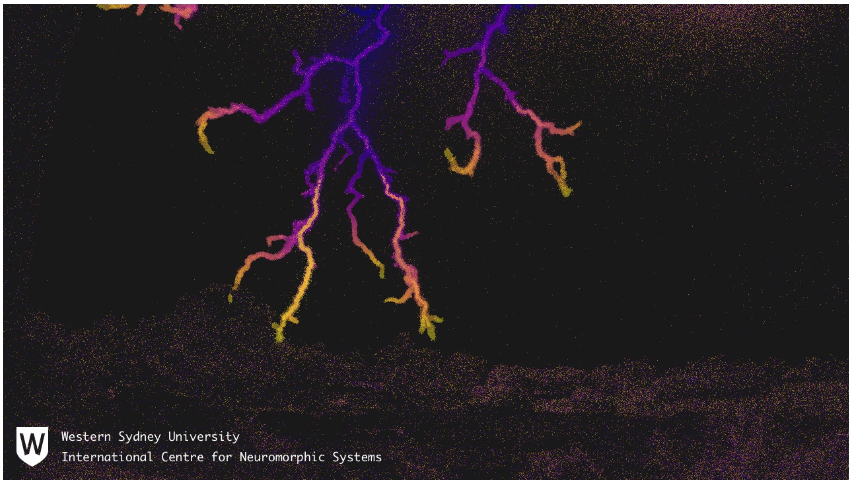

(b) Rainbow plot with temporal range of 0.0 to 0.009412 seconds; right before the return stroke initiation.

Figure 3: Event-rate plot and rainbow plot of a lightning flash with a single return stroke

the two return stroke sequences, there are minor peaks at around 0.178500 seconds after the flash initiation and when the first RS sequence died off. From their magnitude, and verification with visual techniques, we can see that these peaks relate to unsuccessful dart leaders in the main channel. Upon examining the total event-rate plot of the lightning flash, Figure 4, we observe up to 10 peaks that correspond to RS. However, many of these return strokes were not as distinct when using our visual processing tools. Moreover, whilst event-rate plots allow further investigation of lightning features, our visualization techniques require improvement to differentiate between dart leaders and return strokes visually for particularly bright strikes that are clustered together.

Captured at around 19:51, lightning flash in figure 5 is a negative branched stepped leader that does not initiate a return stroke. The unsuccessful leader does not progress far from the cloud until its propagation halts. Following the initial propagation is a series of luminous events traveling up and down the initial main propagation path. The reionization of the plasma channel indicates recoil activity, corresponding to local small peaks within the event-rate plot of magnitude below 10^7. The event-rate magnitude from the background noise prior to the leader was between 10^5 and 10^6. In both the event-

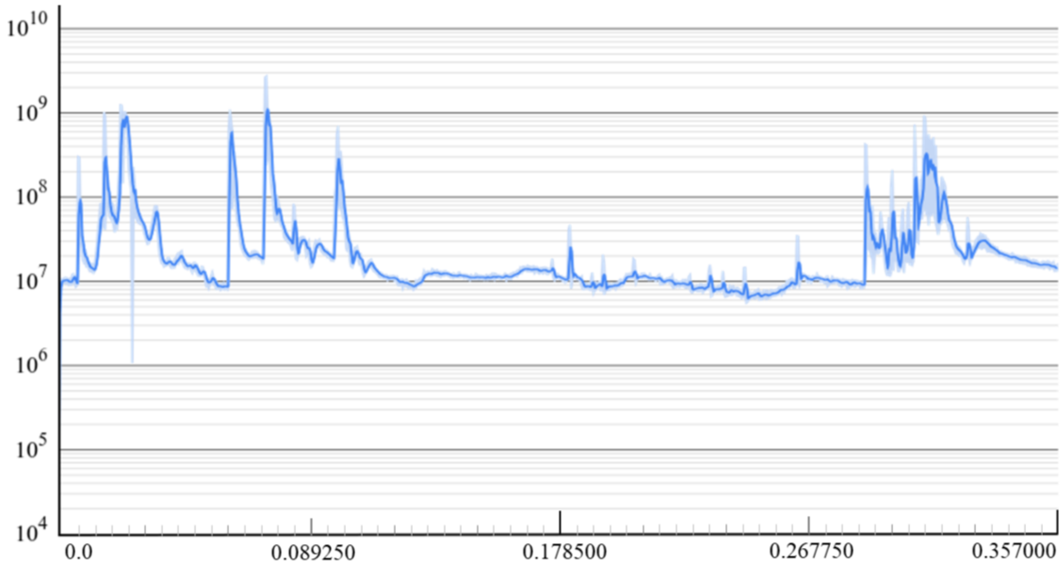

Figure 4: Events over time (seconds) of a lightning flash with several return strokes and dart leaders

based video and the event-rate plot of this lightning flash, there is no evidence of a return stroke.

3.2 Time-Dimension Plots

Figure 6 features a CC lightning strike. Using a rainbow plot, we can select features of a strike, visualizing its start to end. Commencing from the top right of the plot (Figure 6b), an initial negative stepped leader propagates across the field of view, branching as it progresses (Figure 6c). The negative leader is followed by a return stroke through the main channel, Figure 6d, and a second return stroke is initiated at a different main channel after the first, Figure 6e. Shortly after these events, a brief, intense, and irregular bright flash occurs within a previously inactive branch channel (Figure 6f).

3.3 Tracking Results

Figure 7 demonstrates the tracking of lightning leaders in the same strike as shown in Figure 6a. DBSCAN is shown here to successfully detect lightning leaders as prominent event clusters in the presence of background noise. The weighted centroid of these clusters was used as position measurements for the GNN tracker. Using this tracking-by-detection approach while observing from a single fixed perspective produces seemingly relative position and speed estimates for lightning leaders in a 2D plane. The tracker assumes a point target model which asserts that targets have no spatial extent, which causes spatially extended phenomena such as return strokes to be poorly tracked as no discernible single point target can be detected by DBSCAN for tracking.

4 Conclusions

4.1 Interpretation of Results

The features captured by the EBVS as presented here largely align with previously published observations with conventional sensors, thereby validating the use of the EBVS

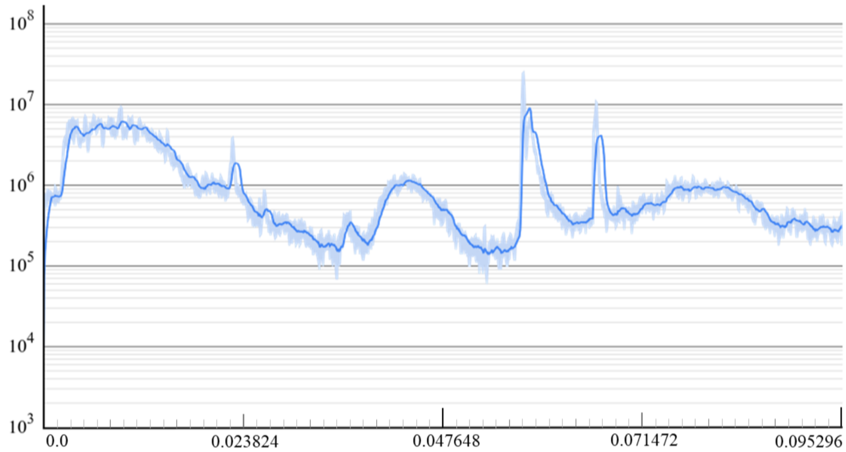

(a) Events over time (seconds)

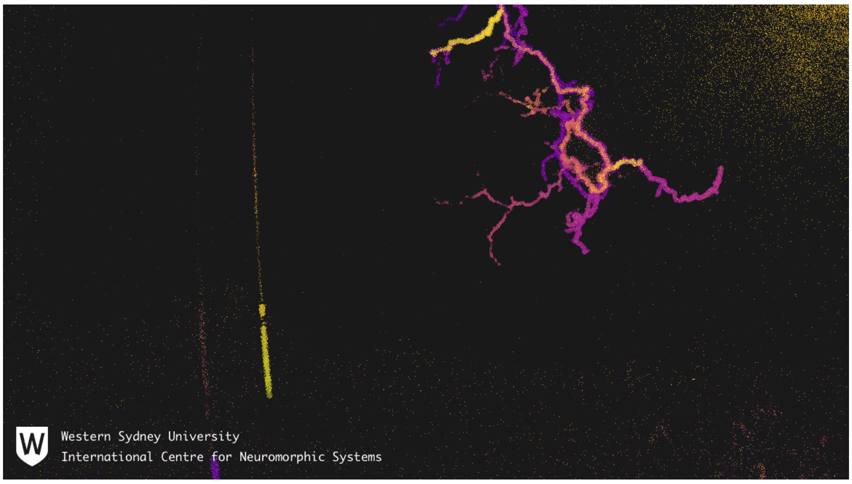

(b) Rainbow plot with temporal range of 0.0 to 0.072310 seconds

Figure 5: Event-rate plot and rainbow plot of a lightning flash with no return stroke but several dart leaders. Note the yellow streak on the left of the image is rain.

as a complementary tool for lightning analysis and may provide improved observations on some features of lightning. The benefits of the EBVS, demonstrated in this paper, include the ability to record a storm from beginning to end, capturing orders of magnitude less data than a comparable high-speed camera, high temporal resolution, portability, and alternative methods of presenting and analyzing the data. The high temporal resolution combined with the sensor's high dynamic range provides opportunities to visualize features of lighting previously unresolved and provide complementary data to high-speed camera observations.

The data analysis techniques available to use on event-based data may also provide new opportunities in capturing features of lightning. The colored rainbow plots demonstrate the ability to add a temporal aspect to static images by adding a color spectrum, an advantage for displaying a lightning strike where it is not possible to publish a video of the strike. Event-rate plots are useful in demonstrating the comparative relative intensities of leaders and are particularly useful in identifying return strokes or discharge activity, aiding in data processing, and capturing elusive information.

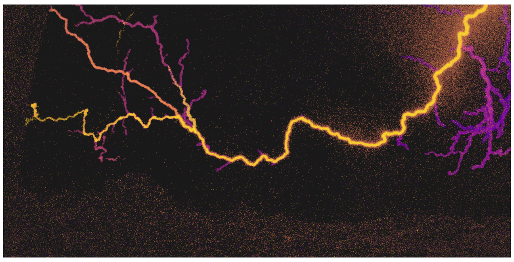

(a) Whole Strike

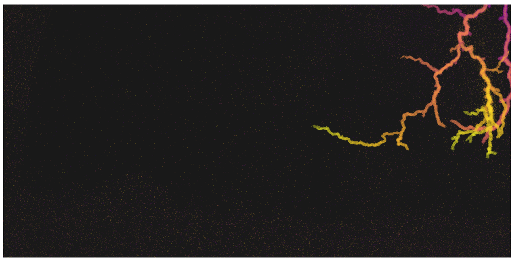

(b) Leader initial propagation

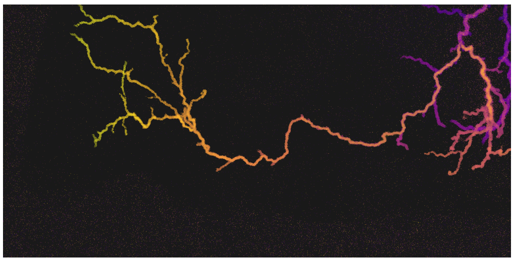

(c) Leader propagation and branching

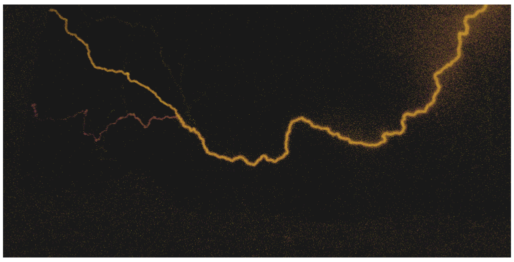

(d) First return stroke

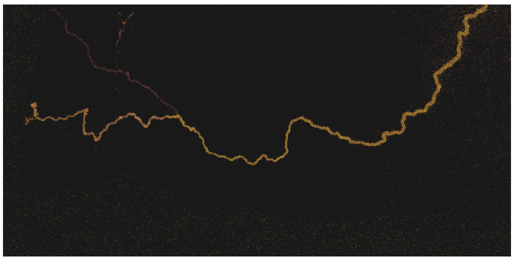

(e) Second return stroke

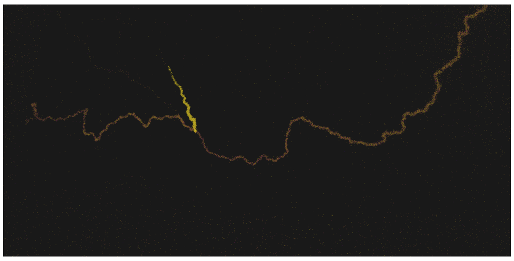

(f) Unusual bright flash

Figure 6: Rainbow plot of a lightning flash, consisting of a negative stepped leader with two main channels that the return strokes pass through and an unusual bright flash through a decayed branch channel after the return strokes.

The results of the tracking algorithm presented illustrate the potential for measuring the speed of lightning leaders. These results show that the high temporal resolution of the EBVS can leveraged to produce similarly high temporal resolution state estimates of specific lightning phenomena. Multiple time synchronized EBVSs are required to track leaders and other phenomena in 3D via depth estimation.

Despite the comprehensive documentation of negative leaders, numerous characteristics remain poorly understood (Dwyer & Uman, 2014). Various theories have emerged regarding leader mechanisms and their subsequent features. In a recent paper, Wang et al. (2022) defined six types of lightning leaders that can initiate a return stroke (RS) or a continuing current (CC) process in negative cloud-to-ground (CG) lightning flashes. Our focus, aligning with most captured lightning strikes, centers on downward negative stepped leaders and downward negative dart leaders. The EBVS provided a clear visualization of full leader propagation, capturing the entire sequence from the initial branching within the cloud to just before the return stroke (for example, Figure 3b). As further branching occurs, it is understood that highly structured and rapidly changing electric field pattern forms, leading to complex interactions between the branches (Ding & Rakov, 2022). As the negative leader propagates downward, we observe a luminous tip with surges of luminosity along the extending branch. Whilst we speculate that this phe-

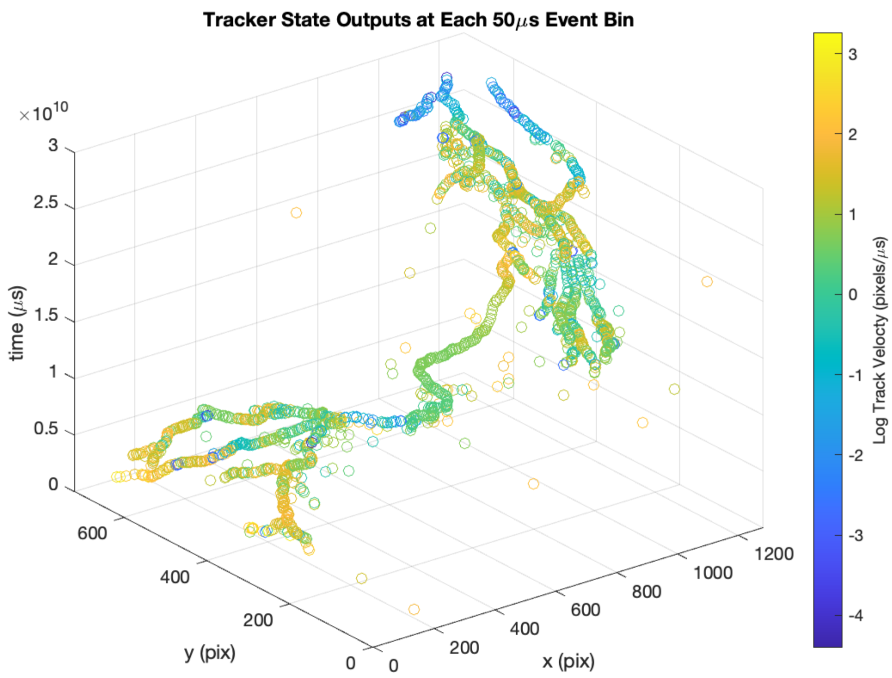

(a)

Figure 7: Trajectory estimates of all confirmed tracks produced by the proposed GNN Tracking algorithm for observation 2023-01-24T19-51-46 in the spatial x, y pixel dimension and time t, colored by log pixel velocity in pixels per μs.

nomenon aligns with Ding and Rakov (2022) description of a negative branched leader generating traveling waves, moving positive charge from the branch tip up along the channel, it requires further investigation in future research.

Return strokes are the result of a conductive hot plasma channel being formed during the attachment process (Liang et al., 2014). This plasma channel is surrounded by a cold plasma charged corona sheath with low conductivity, whose charge is subsequently neutralized when a current wave travels upward from the ground (the negative return stroke) and emits intense optical radiation (Liang et al., 2014). The extremely bright return stroke propagates upward along the main channel at velocity around one-third the speed of light (Liang et al., 2014; Zhou et al., 2019; Dwyer & Uman, 2014). As the EBVS makes use of independent and asynchronous analogue pixels, these sensors can leverage their high dynamic range (both within each pixel, and across the array of pixels) to capture the intense intense optical radiation was clearly detected in our results. The event-rate plot shows clear spikes corresponding with the lightning leaders initiating return strokes. This proved useful, particularly since observing the complete return stroke for each lightning strike in the sensor footage posed challenges due to the extremely rapid and luminous nature of the return strokes. Additionally, the path of the extremely bright return stroke in some instances could be traced using the off-events that remained after, which can be visualised in post-processing of the data. Furthermore, in certain instances, the trajectory of exceptionally intense return stroke could be discerned by following the residual off-events. In these off-events, there are instances where the outward shock wave that occurs immediately after the return stroke is clearly visible.

After the first return stroke, leaders may follow the main channel's path, often called dart leaders. The mechanism by which dart leaders navigate through apparently dormant plasma channels is not well understood (Dwyer & Uman, 2014; B. M. Hare et al., 2023). It is understood that negative charge is propelled forward in the form of a corona streamer zone primarily guided by the existing warm channel, whilst simultaneously, positive charge is introduced into the hot core behind the tip and travels backward toward the cloud charge source (Ding & Rakov, 2022). While discerning the dart leader's travel direction at each instance captured by the EBVS is challenging, our recordings depict its travel both upward and downward along the main channel following the downward negative stepped lightning leader. However, in negative CG lightning flashes, most reported dart leaders propagate downward from the cloud to initiate subsequent return strokes in both downward and upward lightning flashes (Wang et al., 2022). Aligning with previous studies, the successive dart leaders observed by the EBVS were observed to have an increased velocity on average (Jensen et al., 2020). The dart leader, if successful, may trigger subsequent return strokes, leading to the occurrence of multiple return strokes within a single lightning sequence. Previous studies have captured instances of multiple return strokes in various cases (Yuan et al., 2020; Shi et al., 2019; Filik et al., 2021). In our observations, we captured multiple natural negative return strokes that closely followed the dart leader. Throughout a sequence of multiple return strokes, there is a broad variation in intensity. However, the general trend indicates a decrease in intensity as successive return strokes traverse the same plasma channel. Despite some variation, the successive return stroke never appears brighter than the initial return stroke initiated by the negative leader.

In certain instances, a dart leader may fail to successfully initiate a return stroke and instead remain within the cloud; here, they are identified as recoil leaders and these phenomena, like dart leaders, is very poorly understood (Jensen et al., 2020; Jiang et al., 2021; Huang et al., 2021; Cruz et al., 2022; Liu et al., 2021; B. M. Hare et al., 2023). In the data presented in this paper, the EBVS captured various instances of recoil leaders both inside and outside the cloud, where the leader is unable to reach the ground and generate a return stroke. Furthermore, we recorded negative lightning leaders that similarly that did not contact the ground or another cloud to facilitate the attachment process crucial for a return stroke, rendering them unsuccessful leaders. Despite lacking a return stroke, these unsuccessful leaders exhibited lightning activity like dart leaders and can be referred to as recoil leaders as they followed the path of the original leader and it's branches. Typically, in such cases, the recoil leader would adhere to a main channel, although activity could also be observed from nearby branches. Understanding of the underlying mechanisms of this process requires further work.

4.2 Limitations and Future Work

Obtaining and understanding quantitative information about lightning from the EBVS is presently challenging, as the use of EBVS in the context of studying lighting is novel, and the lack of publicly available research into the exact number of photons required to activate a pixel. our current understanding of how the sensor precisely reacts to and interacts with individual photons is incomplete. Consequently, measuring physical properties of lightning, such as luminance, is currently not possible with the current generation of sensors (Gallego et al., 2020). Nevertheless, qualitative information can still be obtained due to the sensor's capabilities of capturing lightning features. The promising results demonstrated in this paper highlight the capabilities of the current generation of sensors. These have not been developed or optimized for lightning detection, and therefore the results demonstrated in this paper represent the baseline performance achievable with this technology.

Future observations will endeavour to use the EBVS in conjunction with other sensors, such as radio frequency detection will allow us to determine the distance to lightning, which in turn may assist in measuring the length and speed of leaders. Furthermore, we are currently testing the EBVS ability to detect spectral lines. Some initial testing shows spectra can be detected when using grating filters. Further testing is required to determine how well the EBVS will see narrow band spectral lines, and if proven possible, we intend to undertake observations attempting to detect spectral lines in lightning using EBVS.

The ability to model lightning captured in the radio spectrum in multiple dimensions has recently been demonstrated by B. Hare et al. (2018) using low-frequency radio observations. They demonstrate a similar result (albeit a different method) to the tracking lightning leaders through the sky as per the results presented in this paper. To expand the potential of our own tracking algorithms, observations of lightning with multiple time-synchronized EBVSs would allow multi-dimensional tracking of leaders spatially, giving direction and speed of leaders, and increases potential to observe other features such as leader tortuosity and behavior between stepping leaders.

Future tracking using the EBVS with lightning data could also benefit from the use of more complex state estimation algorithms such as multi-hypothesis tracking (Blackman, 2004) or probability hypothesis density filtering (Vo & Ma, 2006), which are more resilient to noise and measurement-to-target association ambiguity. Additionally, the point-target model assumption could be relaxed for more robust tracking of phenomena such as return strokes which have a large and non-uniform spatial extent.

There is also potential for the data presented in this work to be further analysed to investigate specific features. There are a multitude of features captured in the data used for this work that have the potential to be investigated further. Some of these features could be allocated to previously understood phenomena of lightning initiation, propagation and re-ignition. Examples of these include, but are not limited to, luminous events accumulating throughout the view of the EBVS before the initial propagation of the negative leader, nature of negative stepped leader initiation and propagation, dart leader propagation and the succeeding return stroke and luminous events within the channel of a lightning discharge event after the discharge occurs.

The potential of the EBVS in furthering understanding of the physical processes of lightning is herein demonstrated. From the conclusions we discuss here, there is significant potential to further investigate a multitude of EBVS features in capturing lightning, and in the analysis of the data itself. To fully exploit this technology, strong collaborations between lightning researchers and neuromorphic researchers to ensure the maximum potential of the EBVS in the study of lightning is achieved.

Acronyms

EBVS Event Based Vision Sensor
CG Cloud-to-Ground lightning
CC Cloud-to-Cloud lightning
DBSCAN Density-Based Spatial Clustering of Applications with Noise
GNN Global Nearest Neighbour
GNNT Global Nearest Neighbour Tracker

Open Research Section

Raw data used in the analysis of this paper can be obtained in .csv form in the Zenodo repository at https://zenodo.org/doi/10.5281/zenodo.10656060 Registration to Zenodo is required to download the data. The data is covered by the Creative Commons licence system.

Acknowledgments

The authors acknowledge the people of the Darug Nation, traditional owners of the land on which the data were collected and research undertaken for this paper.

References

Biagi, C. J., Jordan, D. M., Uman, M. A., Hill, J. D., Beasley, W. H., & Howard, J. (2009). High-speed video observations of rocket-and-wire initiated lightning. *Geophysical Research Letters*, *36*(15). Retrieved from `https://agupubs.onlinelibrary.wiley.com/doi/abs/10.1029/2009GL038525` doi: https://doi.org/10.1029/2009GL038525

Biagi, C. J., Uman, M. A., Hill, J. D., & Jordan, D. M. (2014). Negative leader step mechanisms observed in altitude triggered lightning. *Journal of Geophysical Research: Atmospheres*, *119*(13), 8160-8168. Retrieved from `https://agupubs.onlinelibrary.wiley.com/doi/abs/10.1002/2013JD020281` doi: https://doi.org/10.1002/2013JD020281

Biagi, C. J., Uman, M. A., Hill, J. D., Jordan, D. M., Rakov, V. A., & Dwyer, J. (2010). Observations of stepping mechanisms in a rocket-and-wire triggered lightning flash. *Journal of Geophysical Research: Atmospheres*, *115*(D23). Retrieved from `https://agupubs.onlinelibrary.wiley.com/doi/abs/10.1029/2010JD014616` doi: https://doi.org/10.1029/2010JD014616

Blackman, S. S. (2004). Multiple hypothesis tracking for multiple target tracking. *IEEE Aerospace and Electronic Systems Magazine*, *19*(1), 5–18.

Blackman, S. S., & Popoli, R. (1999). Design and analysis of modern tracking systems. *(No Title)*.

Cai, L., Chu, W., Wang, J., Zhou, M., Yan, Y., Tian, R., & Fan, Y. (2022). Observation and modeling of dart leader development in an altitude-triggered lightning flash. *Journal of Geophysical Research: Atmospheres*, *127*(24), e2022JD037545. Retrieved from `https://agupubs.onlinelibrary.wiley.com/doi/abs/10.1029/2022JD037545` (e2022JD037545 2022JD037545) doi: https://doi.org/10.1029/2022JD037545

Campos, L. Z., Saba, M. M., Warner, T. A., Pinto, O., Krider, E. P., & Orville, R. E. (2014). High-speed video observations of natural cloud-to-ground lightning leaders – a statistical analysis. *Atmospheric Research*, *135-136*, 285-305. Retrieved from `https://www.sciencedirect.com/science/article/pii/S0169809513000057` doi: https://doi.org/10.1016/j.atmosres.2012.12.011

Cruz, I. T., Saba, M. M. F., Schumann, C., & Warner, T. A. (2022). Upward bipolar lightning flashes originated from the connection of recoil leaders with intracloud lightning. *Geophysical Research Letters*, *49*(22), e2022GL101072. Retrieved from `https://agupubs.onlinelibrary.wiley.com/doi/abs/10.1029/2022GL101072` (e2022GL101072 2022GL101072) doi: https://doi.org/10.1029/2022GL101072

Del Moral, P. (1997). Nonlinear filtering: Interacting particle resolution. *Comptes Rendus de l'Académie des Sciences-Series I-Mathematics*, *325*(6), 653–658.

Ding, Z., & Rakov, V. A. (2022). Toward a better understanding of negative lightning stepped leaders. *Electric Power Systems Research*, *209*, 108043. Retrieved from `https://www.sciencedirect.com/science/article/pii/S0378779622002681` doi: https://doi.org/10.1016/j.epsr.2022.108043

Dwyer, J. R., & Uman, M. A. (2014). The physics of lightning. *Physics Reports*, *534*(4), 147-241. Retrieved from `https://www.sciencedirect.com/science/article/pii/S037015731300375X` (The Physics of Lightning) doi: https://doi.org/10.1016/j.physrep.2013.09.004

Ester, M., Kriegel, H.-P., Sander, J., Xu, X., et al. (1996). A density-based algorithm for discovering clusters in large spatial databases with noise. In *kdd* (Vol. 96, pp. 226–231).

Filik, K., Hajder, S., & Masłowski, G. (2021, Apr). Multi-stroke lightning interaction with wiring harness: Experimental tests and modelling. *Energies*, *14*(8), 2106. Retrieved from `http://dx.doi.org/10.3390/en14082106` doi: 10.3390/en14082106

Gallego, G., Delbrück, T., Orchard, G., Bartolozzi, C., Taba, B., Censi, A., ... others (2020). Event-based vision: A survey. *IEEE transactions on pattern analysis and machine intelligence*, *44*(1), 154–180.

Gamerota, W. R., Idone, V. P., Uman, M. A., Ngin, T., Pilkey, J. T., & Jordan, D. M. (2014). Dart-stepped-leader step formation in triggered lightning. *Geophysical Research Letters*, *41*(6), 2204-2211. Retrieved from `https://agupubs.onlinelibrary.wiley.com/doi/abs/10.1002/2014GL059627` doi: https://doi.org/10.1002/2014GL059627

Hare, B., Scholten, O., Bonardi, A., Buitink, S., Corstanje, A., Ebert, U., ... others (2018). Lofar lightning imaging: Mapping lightning with nanosecond precision. *Journal of Geophysical Research: Atmospheres*, *123*(5), 2861–2876.

Hare, B. M., Scholten, O., Buitink, S., Dwyer, J. R., Liu, N., Sterpka, C., & ter Veen, S. (2023, Jan). Characteristics of recoil leaders as observed by lofar. *Phys. Rev. D*, *107*, 023025. Retrieved from `https://link.aps.org/doi/10.1103/PhysRevD.107.023025` doi: 10.1103/PhysRevD.107.023025

Hare, B. M., Scholten, O., Dwyer, J., Ebert, U., Nijdam, S., Bonardi, A., ... Winchen, T. (2020, Mar). Radio emission reveals inner meter-scale structure of negative lightning leader steps. *Phys. Rev. Lett.*, *124*, 105101. Retrieved from `https://link.aps.org/doi/10.1103/PhysRevLett.124.105101` doi: 10.1103/PhysRevLett.124.105101

Hill, J. D., Uman, M. A., & Jordan, D. M. (2011). High-speed video observations of a lightning stepped leader. *Journal of Geophysical Research: Atmospheres*, *116*(D16). Retrieved from `https://agupubs.onlinelibrary.wiley.com/doi/abs/10.1029/2011JD015818` doi: https://doi.org/10.1029/2011JD015818

Huang, H., Wang, D., Wu, T., & Takagi, N. (2021). Recoil leader and associated discharge features observed during the progression of a multi-branched upward lightning flash. *Journal of Geophysical Research: Atmospheres*, *126*(24), e2021JD035162. Retrieved from `https://agupubs.onlinelibrary.wiley.com/doi/abs/10.1029/2021JD035162` (e2021JD035162 2021JD035162) doi: https://doi.org/10.1029/2021JD035162

Jensen, D., Sonnenfeld, R. G., Stanley, M. A., Edens, H. E., da Silva, C. L., & Krehbiel, P. R. (2020, dec). Dart-leader and k-leader velocity from initiation site to termination time-resolved with 3d interferometry. Retrieved from `https://doi.org/10.1002%2Fessoar.10505017.1` doi: 10.1002/essoar.10505017.1

Jiang, R., Qie, X., Wang, Z., Zhang, H., Lu, G., Sun, Z., ... Li, X. (2015). Characteristics of lightning leader propagation and ground attachment. *Journal of Geophysical Research: Atmospheres*, *120*(23), 11,988-12,002. Retrieved from `https://agupubs.onlinelibrary.wiley.com/doi/abs/10.1002/2015JD023519` doi: https://doi.org/10.1002/2015JD023519

Jiang, R., Yuan, S., Qie, X., Liu, M., & Wang, D. (2021). Activation of abundant recoil leaders and their promotion effect on the negative-end breakdown in an intracloud lightning flash. *Geophysical Research Letters*, *49*(1), e2021GL096846. Retrieved from `https://agupubs.onlinelibrary.wiley.com/doi/abs/10.1029/2021GL096846` (e2021GL096846 2021GL096846) doi: https://doi.org/10.1029/2021GL096846

Kalman, R. E. (1960). A new approach to linear filtering and prediction problems.

Liang, C., Carlson, B., Lehtinen, N., Cohen, M., Marshall, R. A., & Inan, U. (2014). Differing current and optical return stroke speeds in lightning. *Geophysical Research Letters*, *41*(7), 2561-2567. Retrieved from `https://agupubs.onlinelibrary.wiley.com/doi/abs/10.1002/2014GL059703` doi:

https://doi.org/10.1002/2014GL059703

Liu, G., Wang, X., Cai, H., Liao, M., Hu, S., & Liu, Y. (2021). Optical characteristics of recoil leader activity in one positive cloud-to-ground lightning flash. In *2021 35th international conference on lightning protection (iclp) and xvi international symposium on lightning protection (sipda)* (Vol. 1, p. 01-06). doi: 10.1109/ICLPandSIPDA54065.2021.9627372

Lowke, J. J., & Szili, E. J. (2022, dec). Toward a theory of 'stepped-leaders' in lightning. *Journal of Physics D: Applied Physics*, *56*(4), 045201. Retrieved from `https://dx.doi.org/10.1088/1361-6463/aca103` doi: 10.1088/1361-6463/aca103

Petersen, D. A., & Beasley, W. H. (2013). High-speed video observations of a natural negative stepped leader and subsequent dart-stepped leader. *Journal of Geophysical Research: Atmospheres*, *118*(21), 12,110-12,119. Retrieved from `https://agupubs.onlinelibrary.wiley.com/doi/abs/10.1002/2013JD019910` doi: https://doi.org/10.1002/2013JD019910

Qi, Q., Lu, W., Ma, Y., Chen, L., Zhang, Y., & Rakov, V. A. (2016). High-speed video observations of the fine structure of a natural negative stepped leader at close distance. *Atmospheric Research*, *178-179*, 260-267. Retrieved from `https://www.sciencedirect.com/science/article/pii/S0169809516300837` doi: https://doi.org/10.1016/j.atmosres.2016.03.027

Qi, Q., Lyu, W., Ma, Y., Wu, B., Chen, L., Jiang, R., ... Rakov, V. A. (2019). High-speed video observations of natural lightning attachment process with framing rates up to half a million frames per second. *Geophysical Research Letters*, *46*(21), 12580-12587. Retrieved from `https://agupubs.onlinelibrary.wiley.com/doi/abs/10.1029/2019GL085072` doi: https://doi.org/10.1029/2019GL085072

Rakov, V. A., Tran, M. D., Zhu, Y., Ding, Z., Leal, A. F. R., Kereszy, I., & Chen, S. (2022, nov). New insights into the lightning discharge processes. *Plasma Sources Science and Technology*, *31*(10), 104005. Retrieved from `https://dx.doi.org/10.1088/1361-6595/ac9330` doi: 10.1088/1361-6595/ac9330

Ralph, N., Joubert, D., Jolley, A., Afshar, S., Tothill, N., van Schaik, A., & Cohen, G. (2022). Real-time event-based unsupervised feature consolidation and tracking for space situational awareness. *Frontiers in neuroscience*, *16*.

Saba, M. M. F., Ballarotti, M. G., & Pinto Jr., O. (2006). Negative cloud-to-ground lightning properties from high-speed video observations. *Journal of Geophysical Research: Atmospheres*, *111*(D3). Retrieved from `https://agupubs.onlinelibrary.wiley.com/doi/abs/10.1029/2005JD006415` doi: https://doi.org/10.1029/2005JD006415

Saraiva, A. C. V., Campos, L. Z. S., Williams, E. R., Zepka, G. S., Alves, J., Pinto Jr., O., ... Blakeslee, R. J. (2014). High-speed video and electromagnetic analysis of two natural bipolar cloud-to-ground lightning flashes. *Journal of Geophysical Research: Atmospheres*, *119*(10), 6105-6127. Retrieved from `https://agupubs.onlinelibrary.wiley.com/doi/abs/10.1002/2013JD020974` doi: https://doi.org/10.1002/2013JD020974

Shi, D., Wang, D., Wu, T., & Takagi, N. (2019). Correlation between the first return stroke of negative cg lightning and its preceding discharge processes. *Journal of Geophysical Research: Atmospheres*, *124*(15), 8501-8510. Retrieved from `https://agupubs.onlinelibrary.wiley.com/doi/abs/10.1029/2019JD030593` doi: https://doi.org/10.1029/2019JD030593

Thiemann, E. M., & Gasiewski, A. J. (2014). Time-domain solution to maxwell's equations for a lightning dart leader and subsequent return stroke. In *2014 united states national committee of ursi national radio science meeting (usnc-ursi nrsm)* (p. 1-1). doi: 10.1109/USNC-URSI-NRSM.2014.6928018

Vo, B.-N., & Ma, W.-K. (2006). The gaussian mixture probability hypothesis density filter. *IEEE Transactions on signal processing*, *54*(11), 4091–4104.

Walker, T. D., & Christian, H. J. (2017). Triggered lightning spectroscopy: Part 1. a qualitative analysis. *Journal of Geophysical Research: Atmospheres*, *122*(15), 8000-8011. Retrieved from `https://agupubs.onlinelibrary.wiley.com/doi/abs/10.1002/2016JD026419` doi: https://doi.org/10.1002/2016JD026419

Walker, T. D., & Christian, H. J. (2019). Triggered lightning spectroscopy: 2. a quantitative analysis. *Journal of Geophysical Research: Atmospheres*, *124*(7), 3930-3942. Retrieved from `https://agupubs.onlinelibrary.wiley.com/doi/abs/10.1029/2018JD029901` doi: https://doi.org/10.1029/2018JD029901

Wang, J., Li, Q., Cai, L., Zhou, M., Fan, Y., Xiao, J., & Šunjerga, A. (2019). Multiple-station measurements of a return-stroke electric field from rocket-triggered lightning at distances of 68–126 km. *IEEE Transactions on Electromagnetic Compatibility*, *61*(2), 440-448. doi: 10.1109/TEMC.2018.2821193

Wang, J., Su, R., Wang, J., Wang, F., Cai, L., Zhao, Y., & Huang, Y. (2022). Observation of five types of leaders contained in a negative triggered lightning. *Scientific Reports*, *12*(1). Retrieved from `https://www.nature.com/articles/s41598-022-10366-x` doi: https://doi.org/10.1038/s41598-022-10366-x

Wu, B., Lyu, W., Qi, Q., Ma, Y., Chen, L., Rakov, V. A., ... Liu, H. (2022). High-speed video observations of needles in a positive cloud-to-ground lightning flash. *Geophysical Research Letters*, *49*(2), e2021GL096546. Retrieved from `https://agupubs.onlinelibrary.wiley.com/doi/abs/10.1029/2021GL096546` (e2021GL096546 2021GL096546) doi: https://doi.org/10.1029/2021GL096546

Yuan, S., Qie, X., Jiang, R., Wang, D., Sun, Z., Srivastava, A., & Williams, E. (2020). Origin of an uncommon multiple-stroke positive cloud-to-ground lightning flash with different terminations. *Journal of Geophysical Research: Atmospheres*, *125*(15), e2019JD032098. Retrieved from `https://agupubs.onlinelibrary.wiley.com/doi/abs/10.1029/2019JD032098` (e2019JD032098 2019JD032098) doi: https://doi.org/10.1029/2019JD032098

Zeng, R., Zhuang, C., Zhou, X., Chen, S., Wang, Z., Yu, Z., & He, J. (2016). Survey of recent progress on lightning and lightning protection research. *High Voltage*, *1*(1), 2-10. Retrieved from `https://ietresearch.onlinelibrary.wiley.com/doi/abs/10.1049/hve.2016.0004` doi: https://doi.org/10.1049/hve.2016.0004

Zhang, Y., Zhang, Y., Xie, M., Zheng, D., & Lu, W. (2014). Characteristics and correlation of return stroke, m component and continuing current for triggered lightning. In *2014 international conference on lightning protection (iclp)* (p. 730-734). doi: 10.1109/ICLP.2014.6973219

Zhou, M., Su, X., Wang, J., Lu, Y., Wang, D., Fan, Y., ... Fan, Y. (2019). On the variation of optical return stroke speed along the bottom of lightning channel. *IEEE Transactions on Electromagnetic Compatibility*, *61*(3), 766-777. doi: 10.1109/TEMC.2019.2916703